EuroEcho-Imaging 2016: Highlights

Julien Magne[1*], Bogdan A. Popescu[2], Chiara Bucciarelli-Ducci[3], Bernard Cosyns[4], Erwan Donal[5], Alessia Gimelli[6], Owen Miller[7], Luigi Badano[8] and Gilbert Habib[9-10].

[1] CHU Limoges, Hôpital Dupuytren, Service Cardiologie, Limoges, F-87042, France ; INSERM 1094, Faculté de médecine de Limoges, 2, rue Marcland, 87000 Limoges, France.
[2] University of Medicine and Pharmacy "Carol Davila" - Euroecolab, Institute of Cardiovascular Diseases "Prof. Dr. C. C. Iliescu", Bucharest, Romania.
[3] Bristol Heart Institute, University of Bristol, Bristol, UK.
[4] UZ Brussel- CVHZ, ICMI 101 Laarbeeklaan 1090 Brussels, Belgium.
[5] CIC-IT 1414, CHU Rennes, Université Rennes 1, Service de Cardiologie, CHU RENNES, France.
[6] Fondazione Toscana/CNR Gabriele Monasterio, Pisa, Italy.
[7] Department of Congenital Heart Disease, Evelina London Children's Hospital, London, United Kingdom.
[8] Department of cardiac, thoracic and vascular sciences, University of Padua School of Medicine, Padua, Italy.
[9] Aix-Marseille Univ, URMITE, Aix Marseille Université UM63, CNRS 7278, IRD 198, INSERM 1095 - IHU - Méditerranée Infection
[10] APHM, La Timone Hospital, Cardiology Department, Marseille France

Corresponding author:

***** CHU Limoges, Hôpital Dupuytren, Service Cardiologie, Limoges, F-87042, France ; INSERM 1094, Faculté de médecine de Limoges, 2, rue Marcland, 87000 Limoges, France

Words count: 5 253

Abstract

The annual meeting of the European Association of Cardiovascular Imaging, EuroEcho-Imaging, was held in Leipzig, Germany, in December 2016. In the present paper, we present a summary of the 'Highlights' session.

Key words: heart failure, heart valve disease, new technologies, cardiac magnetic resonance, congenital heart disease, nuclear cardiology, cardiac computed tomography

The twentieth annual scientific meeting of the European Association of Cardiovascular Imaging (EACVI), EuroEcho-Imaging 2016, was held in Leipzig, Germany. The main themes were ‘imaging in arrhythmias’ and ‘aortic valve diseases’.

The meeting was a great success with a high number of participants with 3250 delegates and over 1154 abstracts and clinical cases submitted. Overall, 112 abstracts and clinical cases were accepted as oral presentation, and 56 moderated posters were presented. Of note, the preferred topics regarding abstracts submission were ‘tissue Doppler and speckle tracking’, ‘heart valves‘, ‘cardiomyopathies’, ‘the imaging examination and quality assessment‘, ‘Ischemic heart disease, ‘stress echo‘, and ‘systemic disease’.

On the last day of the meeting, the ‘Highlights’ session wrapped up the event with a summary of the most relevant abstracts presented throughout the congress. A short report of this session is presented below.

Heart Failure

Myocardial Shear Wave Imaging (SWI) has been investigated to non-invasively quantify the passive diastolic myocardial stiffness in adult. Positive correlations were found between the evaluation of shear wave stiffness (by ultrafast imaging) and clinical parameters and cardiac magnetic resonance parameters, such as native T1-mapping. Non-invasive SWI evaluation of diastolic myocardial stiffness could thus be used more extensively in clinical practice considering platform able to generate the ultrafast imaging technique (1).

The transition from diastole to systole is not a mere shift between the two distinct phases, but rather a continuous process in which intra-cardiac flows form vortices help redirection and blood ejection. The incremental value of left ventricular (LV) vortex flow in predicting clinical outcomes in heart failure has been investigated (2). The vortex formation during isovolumetric contraction, an important mechanism of flow coupling between diastole and

systole, has thus been demonstrated to be associated with clinical outcomes in patients with dilated cardiomyopathy (Figure 1).

Simpler and largely available tools have also been tested to improve diagnosis, management and prognosis of heart failure patients. The alveolar capillary barrier (ACB) integrity can be variably compromised in heart failure patients determining vulnerability to life-threatening pulmonary edema during volume or pressure challenges: the higher the lung permeability, the greater the risk of pulmonary edema during volume expansion and/or pressure rise. Extravascular lung water was assessed with lung ultrasound (LUS) and pulmonary capillary wedge pressure (PCWP) was derived from Doppler and tissue Doppler during exercise stress echocardiography (ESE). Standard transthoracic echocardiography (TTE) and LUS evaluation at rest and at peak semi-supine ESE in 103 NYHA class I-III HF patients with depressed left ventricular ejection fraction have been performed. The slope of the pressure-water relation is highly heterogeneous, ranging from low permeability (flat slope) to steep, high permeability pattern, allowing to recognize the underlying integrity of ACB in HF patients. The overall B-lines number increased from 5 to 10 and to 12 to 45 ($p<0.0001$, peak stress vs. rest). Authors reached to the clinical relevant conclusion that ACB stress is feasible during ESE with a combination of LUS and TTE allowing a simultaneous assessment of lung water and pulmonary wedge pressure (3).

In arrhythmogenic right ventricular cardiomyopathy (ARVC), electrical abnormalities precede overt structural disease. Abnormal RV deformation has been reported in early ARVC without structural abnormalities. ARVC-mutation carriers (n=84) were evaluated (4). Three distinctive characteristic RV longitudinal deformation patterns were identified: Type-I: normal deformation (n=12), Type-II: delayed onset of shortening, reduced systolic peak strain, and mild post-systolic shortening (n=35), and Type-III: systolic stretching with large post-systolic shortening (n=37). A majority (69%) of structural staged mutation carriers

showed Type-III, whereas a large proportion of both electrical and subclinical stage subjects (67% and 48%, respectively) showed Type-II. CircAdapt model simulations demonstrated that the Type-II pattern can be explained by a combination of mildly reduced contractility and increased passive myocardial stiffness. None of the patterns could be explained by an electrical activation delay only. This new application of longitudinal strain imaging could lead to earlier disease detection and thereby influence current definitions of electrical and subclinical ARVC stages.

Another study related to electrophysiology has been presented (5). Frequent premature ventricular contractions (PVCs) may induce a cardiomyopathy. A PVC burden of 24% (approx. 24000 PVCs/24 hours) has previously been related to reduced LV ejection fraction (EF). The authors aimed to explore the threshold number of PVCs inducing LV systolic dysfunction. They included 52 consecutive patients (58% of female) with no overt heart disease. Median %PVC was 7.2 (0.2-60) and %PVC correlated with LV global longitudinal strain (r=0.44, p=0.002) and LV end-diastolic diameter (r=0.32, p=0.02), but not with LVEF (r=0.22, p=0.12). The %PVC >8 accurately identified patients with GLS worse than -18%. This study reached to the conclusion that %PVC correlated with longitudinal systolic function but not significantly with LVEF. GLS detected systolic dysfunction at a lower threshold

New technologies

Hjertaas et al. aimed to construct a LV rotating phantom (Figure 2) for the evaluation of accuracy of 3D speckle tracking echocardiography (STE) twist measurements and to test the impact of different volume rates on 3D twist measurements. The phantom was able to simulate LV twist and could be used to study the effect of volume rate on twist measurements. A range of volume rates provided good agreement with sonomicrometry. Real time and high volume rates gave less accurate twist measurements caused by a reduced beam density. (6)

The second study was rewarded with the clinical young investigator award: a patient-specific numerical model of the mitral valve (MV) apparatus was developed, based on 3D transoesophageal echocardiography (3D-TEE), and evaluated its clinical potential in patients with secondary mitral regurgitation (MR). MV modeling allowed a realistic prediction of valvular closure in normal valves as well as in secondary MR. Predicted geometric determinants of secondary MR correlated with MR severity. Patient-specific numerical MV modeling showed potential for improving mechanistic insights and enhancing therapeutic efficacy by enabling pre-procedural planning and simulation. (7)

Chen et al. examined the mitral annular (MA) dynamicity and compare the surgical effect to annulus dynamicity in different stages of myxomatous mitral valve disease (MMVD) with severe MR. They showed that the MA saddle shape was preserved in early stage of MMVD. Following MV repair (i.e. with annuloplasty), the annular dynamicity was normalized without disrupting the MA saddle shape in early severe MR. The systolic annulus of decompensated group was flat and could not be corrected by annuloplasty. (8)

Another study sought to evaluate the determinants of MA size in a large group of patients with a wide range of LA and LV volume from various diseases in 120 patients who underwent a clinically indicated 3D-TEE. They demonstrated that LA volume appeared as the main determinant of MA size measured using 3D-TEE. Primary MR was the second determinant of MA area suggesting an intrinsic annulus disease. In contrast, LV size had a modest influence on MA size. (9)

Surkova et al. investigated the correlations between the tricuspid annulus (TA) area and right ventricle (RV) and right atrial (RA) volumes in patients with different mechanisms of functional tricuspid regurgitation (F-TR) using 3D-TTE. They showed that RA size is the most consistent determinant of TA dilatation in patients with different mechanisms of F-TR. (10)

A study from UK looked at the RA function evaluated with 3D-STE and its relationship with outcome in patients with different types of pulmonary hypertension (PH). They demonstrated that RA global circumferential strain (GCS) was correlated with RA and RV function. This parameter could be a useful tool for differentiating patients with PH and worse prognosis. (11) Similarly, Peluso et al. investigated the mechanics of RV by 3DE in PH patients, concluding that the radial component of RV wall displacement was as important as the longitudinal to determine global RV pump function. In patients with PH, the impairment of RV pump function was mainly driven by the progressive reduction of RV radial displacement (12).

Heart valve diseases

'Heart valve disease' is always one of the most popular topic at EuroEcho Imaging, and aortic stenosis (AS) remains the most frequently studied disease. Aiming at identify the ideal parameter, among various imaging modalities, allowing to assess myocardial fibrosis in AS, Park et al. (13) studied 87 patients, with preserved LVEF and no significant coronary artery disease or previous history of myocardial infarction, using both CMR and TTE. All patients underwent aortic valve replacement (AVR) and 71 of them had myocardial biopsy at the basal LV septum. From tissue specimen, quantification of myocardial fibrosis area was performed by positive pixel count algorithm using the Aperio ImageScope software. Their results may be summarized as follow:

(1) Various degree of myocardial fibrosis can be found in patients with severe AS

(2) Extracellular volume, derived from CMR T1-mapping, and LV GLS, derived from 2D speckle tracking TTE, were significantly correlated with myocardial fibrosis

(3) Extracellular volume and LV GLS were well correlated ($r=0.666$, $p<0.001$).

These data suggest that LV GLS and particularly extracellular volume could be promising surrogate markers predicting diffuse myocardial fibrosis in patients AS.

The clinical usefulness of computed tomography-derived (CT) calcium score has been extensively studied in patients with AS. However, there is no objective echocardiographic assessment of calcium load available. Gillis et al. (14) aimed to develop an ultrasound global calcium score, based on gray-scale value of TTE (i.e. video intensity), from multiple region of interest in both parasternal short- and long-axis views (Figure 3). They prospectively enrolled 25 patients (32% of male) with various degrees of aortic valve calcification who underwent calcium score quantification using both a cardiac CT and TTE. They reported good correlation between the ultrasound calcium score and CT Agatston score (r^2= 0.4, p=0.0013). In addition, an ultrasound calcium score = 47 units provided 82% sensitivity and 75% specificity for diagnosis of severe calcification, as assessed using CT. Consistently, they concluded that this new ultrasound calcium scoring method represents an interesting, non-ionizing alternative to CT for calcification quantification and localization, and is potentially useful for serial follow-up of patients with AS.

In patients with heart valve disease, the role of RV function has been recently well emphasized, more particularly in patients with primary MR. Vittel et al. (15) aimed to identify whether exercise RV function could be accurate parameters to identify high-risk patients. They prospectively studied 152 patients with no or mild symptoms and with severe primary MR. These patients underwent exercise stress TTE including measurement of tricuspid annular plane systolic excursion (TAPSE) at sub-maximal load. Exercise RV dysfunction was defined as exercise TAPSE<26mm. During a mean postoperative follow-up of 18±26 months, 48 patients (34%) experienced a predefined cardiovascular end-point. Of interest, patients with exercise RV dysfunction had significantly lower cardiac event-free survival (p=0.004) and this relationship remained significant after adjustment for cofactors (p=0.03). The Authors concluded that dynamic assessment of RV function using exercise TAPSE may be

useful for the risk stratification and the management of asymptomatic patients with severe primary MR.

Congenital heart disease

The Congenital Heart Disease (CHD) programme at EuroEcho Imaging 2016 was a mix of the latest science and imaging in clinical practice. The main themes emerging from the oral presentations and posters included left heart problems (aortic & LV disease), Tetralogy of Fallot and single ventricle palliation.

Mas-Stachurska et al. (16) presented results from an experimental model of Marfan's syndrome where both affected and control animals were subjected to regular exercise training. Trained animals had significantly less aortic dilatation and less myocardial pressure overload, suggesting that absolute exercise restriction in Marfan's disease may not be beneficial.

Anomalous Coronary Artery for the Pulmonary Artery (ALCAPA) is a rare but important congenital cause of severe LV dysfunction. Surgical re-implantation may correct gross systolic function as measured by standard parameters. Di Salvo et al. (17) described a more detailed evaluation of LV mechanics using deformation imaging. Although LVEF was comparable between patients and controls, GLS was significantly lower in ALCAPA (-17.6±3.5% vs. -23.4±3.1%, $p<0.0001$), LV torsion was reduced (9.1±4.9° vs. 11.9±3.3°, $p=0.046$) and diastolic parameters [E/e' ratio 11.9±5.8 vs. 6.6±3.0, $p=0.0014$) were abnormal.

With regard to critical left heart obstruction, Mertens et al. (18) reported the initial output from a large multicentre post-hoc analysis of the pre-intervention morphologic and functional echocardiographic characteristics of 651 neonates between 2005-2013. Bonello et al. (19) described a 40-year cohort of patients with treated critical AS. Late follow-up with cardiovascular pulmonary exercise testing (CPET) showed a decrease in peak VO2 over time. Echocardiography and CMR confirmed preserved LVEF but clear evidence of endocardial fibroelastosis (EFE) in 52%. EFE was associated with early Ross intervention (r=-0.52,

p=0.0324), LV diastolic dysfunction (r=-0.48, p=0.0164) and PH (r=0.65, p=0.0004). Almeida-Moras et al. (20) described a more cost effective screen for recurrent coarctation using ESE with a transisthmic gradient elevation from baseline to peak exercise greater than 16.5 mmHg was found to be a sensitive (89%) discriminator compared to the gold standard of CMR.

Pulmonary regurgitation in adults with repaired Tetralogy remains a management dilemma. Pagourelias et al. (21) reported the role of echocardiographic and CMR pre and post Melody valve insertion to guide the decision-making process about the timing of percutaneous pulmonary valve insertion. Using a multimodality approach in asymptomatic patients, intervention less than 7 years after initial repair led to superior remodelling and improved function as measured by longitudinal function and strain analysis. Morillas et al. (22) presented similar results after surgical pulmonary valve replacement (PVR) with improved remodelling if the PVR was undertaken in patients with higher baseline LVEF.

Finally, in single ventricle palliation Fontan patients, Rossner et al. (23) presented an analysis of the increased risk represented by classic pattern dyssynchrony (CPD) in various morphological subtypes undergoing Fontan surgery. They further described how an increased sphericity index associated with some forms of CHD was associated with reduced circumferential strain (Figure 4).

The CHD programme at EuroEcho Imaging continues to strengthen with multimodality integration, pivotal to diagnosis and management.

Nuclear Cardiology and Cardiac Computed Tomography

Perfusion imaging by single-photon emission computed tomography (SPECT) or positron emission tomography (PET) is a robust stress imaging modality in patients with suspected or known coronary artery disease (CAD) due to its well-demonstrated prognostic value. However, up to now, it is not clear whether ischemia burden on stress SPECT effectively

identifies patients who have a long-term benefit from coronary revascularization. To this purpose, Boiten and colleagues (24) retrospectively evaluated the impact of coronary revascularization on long-term outcomes in 719 patients with ischemia at SPECT. The Authors concluded that patients with myocardial ischemia on stress SPECT who underwent early revascularization had a lower all-cause mortality and cardiac mortality during long-term follow up as compared to patients who received pharmacological therapy alone. This difference in long-term outcomes was mainly caused by the survival benefit of early revascularization in the patients with moderate to high ischemia burden.

Another interesting study related to myocardial ischemia was the one presented by Valente and colleagues (25) on coronary CT angiography. The Authors evaluated in 50 patients (no previously known CAD, mean pretest probability of CAD 56%) the diagnostic accuracy of dipyridamole stress dual-energy CT myocardial perfusion plus CT angiography to correctly identify obstructive CAD, as defined by invasive coronary angiography and SPECT, and indication for revascularization. The Authors concluded that dipyridamole stress dual energy CT myocardial perfusion plus CT angiograph allowed correct detection of obstructive CAD when compared with invasive coronary angiography and SPECT. Even if confirmation with further studies is needed, clinical practice implementation of this single test for anatomic and functional evaluation of myocardial ischemia may result in better resource management and in avoidance of unnecessary invasive coronary angiography.

An original application of nuclear imaging is coming from the hypothesis that in dilated LV with a more spherical shape and displaced papillary muscles (PM), the altered geometry may influence the contribution of PM to LV function. To this purpose, Duchenne and colleagues (26) evaluated regional myocardial work by measuring the myocardial glucose uptake by 18-fluorodeoxyglucose (FDG) PET in an animal model of normal and dilated LVs. Fifteen animals were included in the study. Ten sheeps were subjected to 8 weeks of rapid pacing

(180 bpm) to induce LV dilatation and five sheeps served as control. CMR was performed in all animals to assess LV volumes, LVEF and LV sphericity index. The MR was graded visually using CMR cine images. The obtained results indicated that PMs contribute more to LV shortening in dilated compared to normal hearts (Figure 5). The Authors suggested that their higher workload was due to geometric abnormalities in dilated LVs, which make PM work mostly perpendicular through the LV rather than parallel to the LV wall. These results are very important because, if confirmed in larger studies, the increased contribution to LV work in dilated hearts may further strengthen the argument of the preservation of PM during mitral valve repair/replacement in dilated cardiomyopathy.

Another exciting new application of nuclear modalities is imaging of transthyretin related (TTR) amyloidosis by 99mTc3,3diphosphono1,2propanodicarboxylic acid (99mTcDPD) scintigraphy. Pradel and colleagues (27) explored the relationship between cardiac uptake by 99mTcDPD scintigraphy and longitudinal myocardial strain assessed by echocardiography in 40 patients with TTR cardiac amyloidosis, in order to assess the impact of 99mTcDPD cardiac uptake on cardiac function. Global and regional 99mTcDPD cardiac uptake was correlated with GLS, derived from TTE, as well as with segmental longitudinal strain ($r=0.490$, $p=0.001$ and $r=0.155$, $p<0.001$, respectively) but not with LVEF ($r=0.097$, $p=0.558$). These results indicate that the information obtained from different cardiac imaging techniques are required in order to be able to detect undiagnosed diseases.

Cardiovascular magnetic resonance

The best CMR abstracts presented at EuroEcho Imaging 2016 mainly focused on new CMR applications in CHD.

Muthusami et al. (28) presented a study on quantitative CMR stress perfusion and interstitial myocardial fibrosis in patients with Kawasaki disease, a condition often complicated by coronary artery aneurysms, stenosis and microvascular disease. The Authors hypothesized

that additional CMR-derived parameters such as myocardial perfusion reserve index (MPRI), interstitial fibrosis (extracellular volume fraction, ECV) and myocardial contractility might provide added value in guiding management. They retrospectively included 19 patients (11.4±4.2 years, range 4-18 years) undergoing stress CMR with adenosine vasodilator stressor and at rest, in addition to native- and post-contrast T1 mapping. They observed that compared to control, perfusion was reduced in Kawasaki patients (1.51±0.78 vs. 2.63±0.96, $p<0.0001$) and that interstitial fibrosis was increased (24.4±4.51% vs. 23±2.66%, $p=0.0005$). The interstitial fibrosis was also greater in territories supplied by severely diseased coronary arteries than in mildly diseased territories (26.53±4.18% vs. 23.69±4.09%, $p=0.05$). The study concluded that some abnormalities are present in segments with non-infarcted normally contracting territories thus reflecting a subclinical involvement of these segments in part explained by the concomitant reduction in myocardial blood flow.

Dux-Santoy et al. (29) presented 2 studies with CMR 4D flow in 86 patients with bicuspid aortic valve (BAV). In the first study they assessed the impact of different BAV phenotypes (right-to-left [RL] BAV n=65, and right-to-non-coronary [RN] BAV, n=21) on different patterns of wall shear stress (WSS) in the ascending aorta. They acquired eight double-oblique planes equally distributed in the ascending aorta between the sinotubular junction and the origin of the brachiocephalic trunk; peak axial and circumferential WSS peak velocity, eccentricity and rotational flow at different aortic levels were evaluated using 3D maps. They demonstrated that RN-BAV phenotype had higher peak velocities and rotational flow. Accordingly, different BAV phenotypes presented different outflow jet direction and different distribution of WSS within the aortic wall. RN-BAV patients presented a maximum WSS from proximal left posterior-to-distal right aortic wall (Figure 6) while the maximum WSS was from left posterior-to-right anterior at proximal-medial levels in RL-BAV patients. They

conclude that these WSS maps could be a useful tool to better understand the pathophysiology of aortic dilatation in patients with different BAV anatomy.

This study was complemented by a second one (30) evaluating in the same patients flow patterns and rotational flow to predict ascending aorta dilatation. They observed that although through-plane (TP) velocity profile was similar in RL-BAV and in RN-BAV patients, in-plane rotational flow was significantly higher in RN-BAV at all aortic levels. In particular, in RL-BAV the outflow jet was right-anterior at the level of the sinotubular junction, with more homogeneous flow profiles in mid and distal ascending aorta. Conversely, RN-BAV patients showed a higher variability in their flow velocity patterns with a first outflow jet posterior peak and a second peak with a lower velocity. Also, in RN-BAV flow velocity patterns shifted from posterior segments at proximal ascending aorta to right-to-right anterior segments in mid-distal ascending aorta. They concluded that RN-BAV phenotype presents more turbulent flow with a predominant initially posterior outflow jet that shifts to right-anteriorly in mid and distal ascending aorta. Thus, RN-BAV patients have a higher in-plane rotational flow at all levels in the ascending aorta than RL-BAV patients, which may explain different patterns of ascending aorta dilatation patterns among different BAV phenotypes.

Hinojar et al. (31) presented normal reference values of left atrial longitudinal and radial deformation using CMR feature tracking (CMR-FT) in a cohort of 70 healthy volunteers. The importance of assessing LA deformation is increasingly recognized and can be assessed with STE. Feature tracking represents a novel CMR post-processing application capable to provide similar data in a previously acquired cine dataset.

CMR-FT was applied to existing 2-, 3-, and 4-chamber view cines, and atrial longitudinal strain (ALS), atrial longitudinal displacement (ALD), atrial radial strain (ARS) and atrial radial displacement (ARD) LA were calculated and reported in all subjects. The LA deformation parameters did not significantly differ between men and women ($p>0.05$ for all).

The Authors also demonstrated high intra- and inter-observer agreements for ALS and ARS values. This is the first study establishing normal reference values of LA strain using CMR-FT, opening the implementation of this novel technique in clinical practice.

Figures Legend

Figure 1: Transthoracic apical view with the parametric imaging of the vortex that can be quantified using an injection of a contrast agent using a dedicated software. The authors looked at the vortex in all the period of the cardiac cycle and observed that the most valuable period to quantify the vortex was the isovolumic contraction time.

Figure 2: The twisting phantom (A) with 6 sonomicrometer crystals (B) arranged in 2 triangles (basal and apical) imaged with 3D probe (C).

Figure 3: Ultrasound global calcium score semi-automated quantification based on gray-scale value of transthoracic echocardiography.

Figure 4: Differences between anatomic lesions. Patients with TA showed lowest sphericity, lower meridional wall stress and higher strain values (A). Patients with unbalanced AV-Canal showed high sphericity, higher wall stress and lower strain values (B).

Figure 5: Increase in relative work contribution of papillary muscles in normal and dilated left ventricle.

Figure 6: Axial and circumferential wall shear stress (WSS) both in right-to-left (RL) and right-to-non-coronary (RN) bicuspid aortic valve (BAV).

Figure 1

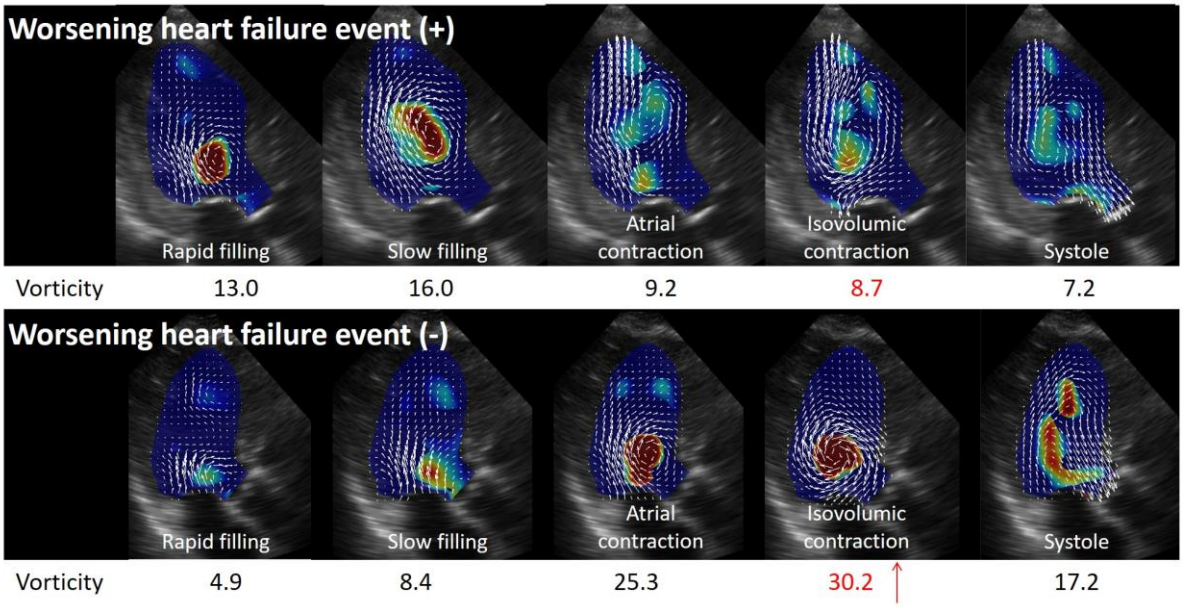
Worsening heart failure event (+)
Rapid filling
Slow filling
Atrial contraction
Isovolumic contraction
Systole
Vorticity
13.0
16.0
9.2
8.7
7.2
Worsening heart failure event (-)
Rapid filling
Slow filling
Atrial contraction
Isovolumic contraction
Systole
Vorticity
4.9
8.4
25.3
30.2
17.2

Figure 2

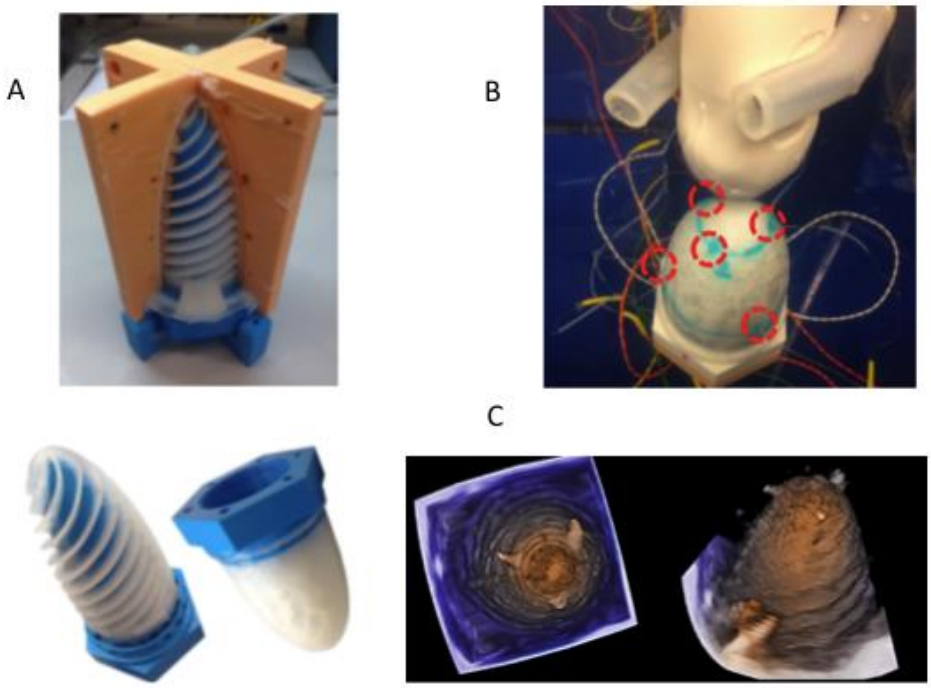

Figure 3

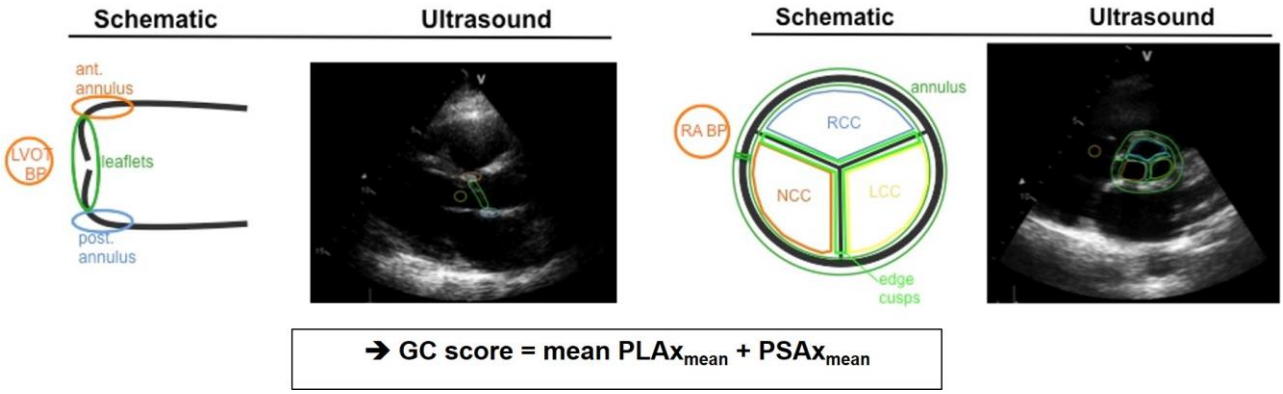
Schematic
Ultrasound
Schematic
Ultrasound
ant. annulus
LVOT BP
leaflets
post. annulus
RA BP
annulus
RCC
NCC
LCC
edge cusps
➔ GC score = mean PLAx$_{mean}$ + PSAx$_{mean}$

Figure 4

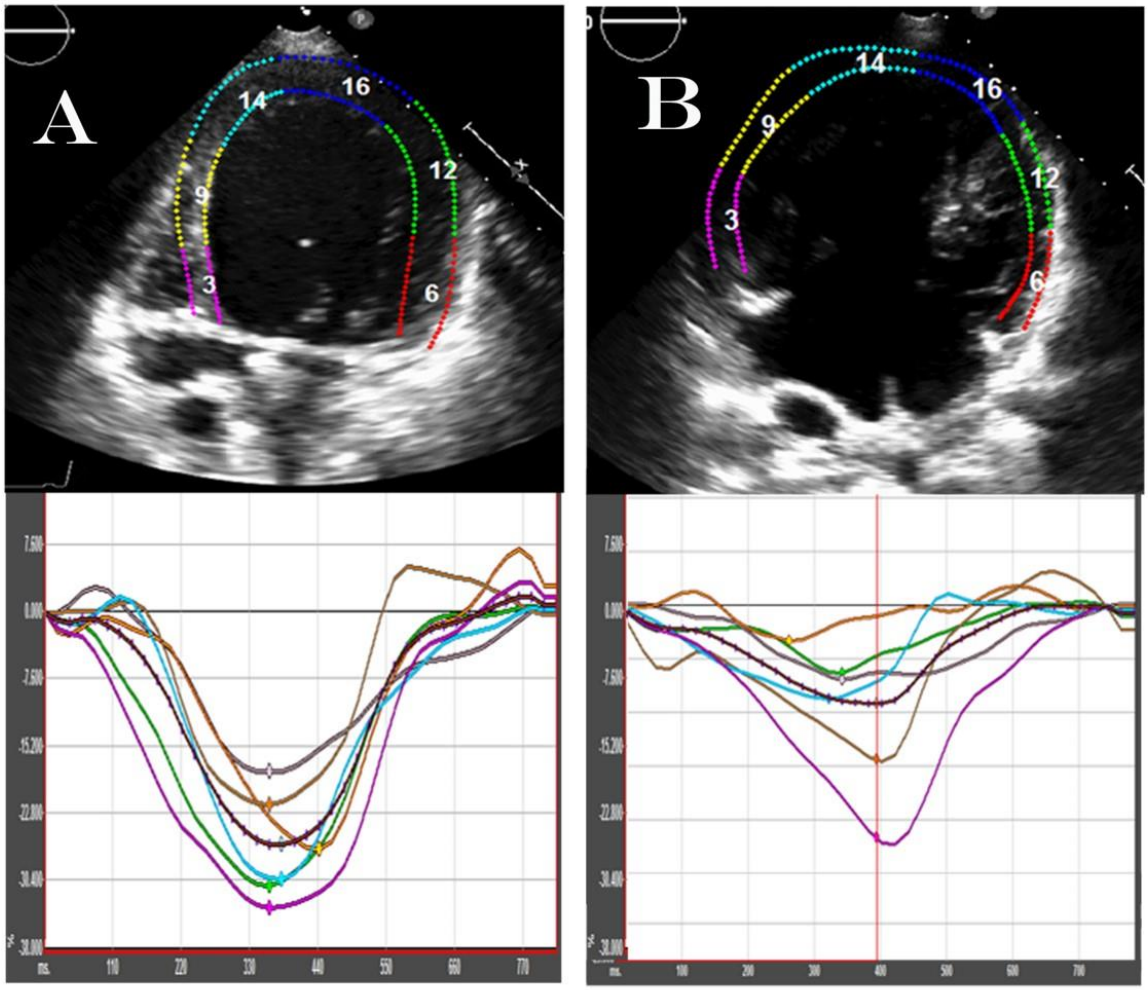

Figure 5

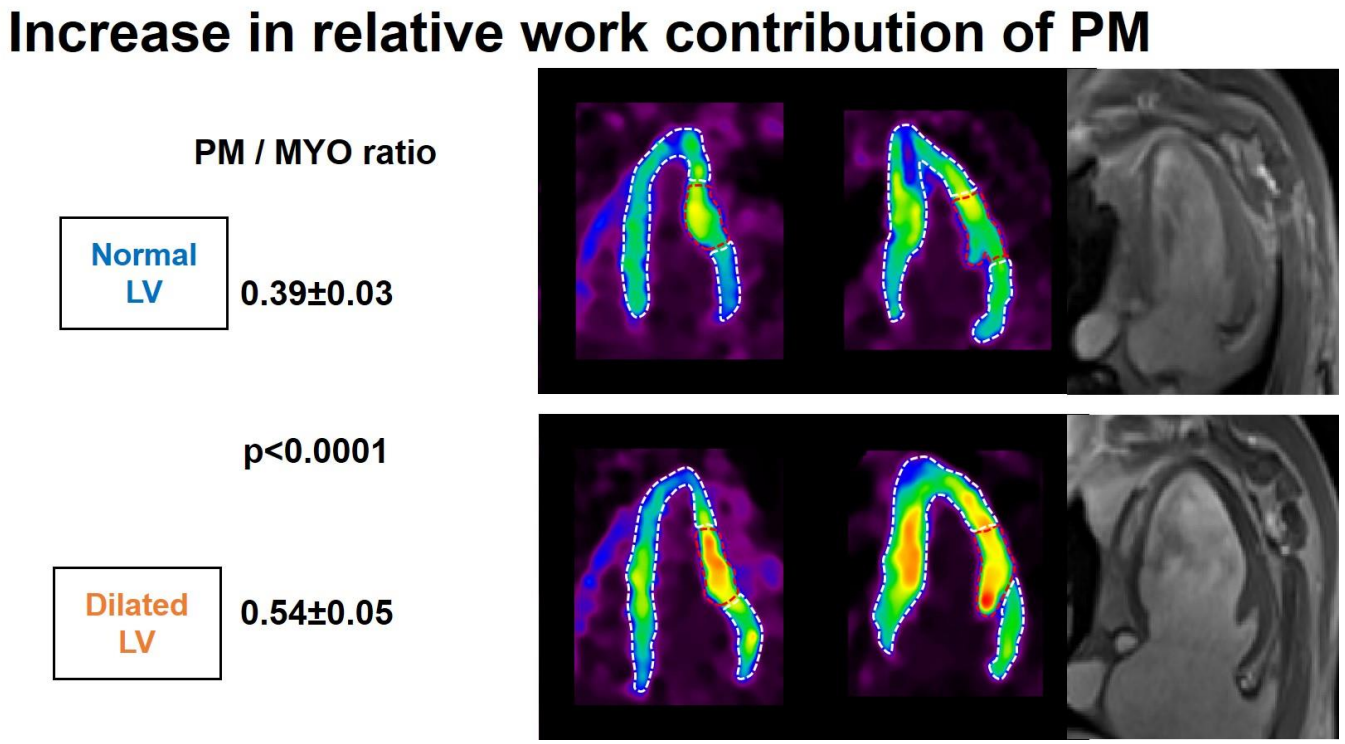
Increase in relative work contribution of PM
PM / MYO ratio
Normal LV
0.39±0.03
p<0.0001
Dilated LV
0.54±0.05

Figure 6

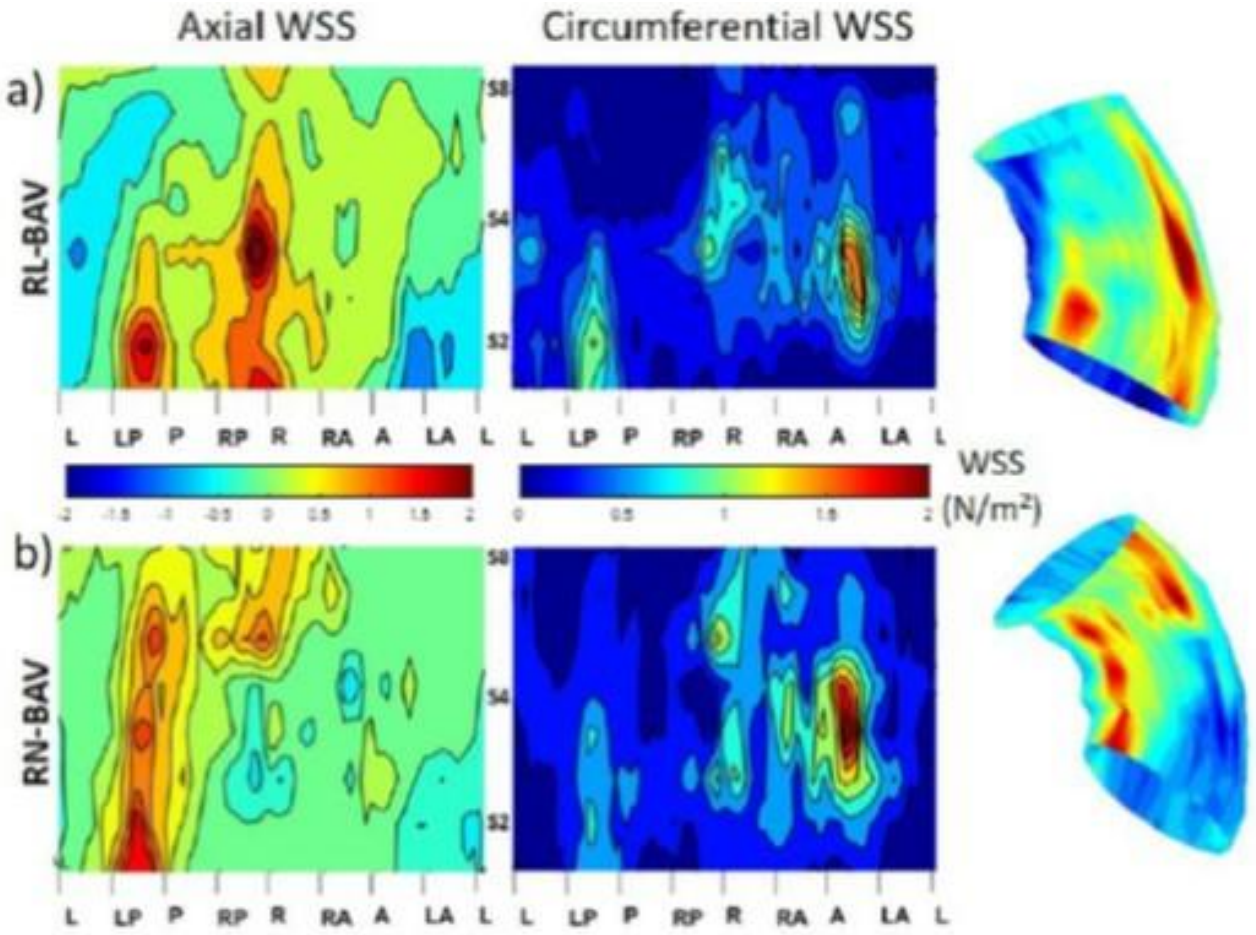
Axial WSS
Circumferential WSS
a)
RL-BAV
b)
RN-BAV
S8
S4
S2
L LP P RP R RA A LA L
WSS
(N/m²)

References list

1. Villemain O, Correia M, Mousseaux E, Baranger J, Zarka S, Pernot M, et al. Myocardial stiffness assessment using shear wave imaging in healthy adult population. Eur Heart J Cardiovasc Imaging 2016 17 (suppl 2): ii49-ii52.
2. Takahashi L, Uejima T, Nishikawa H, Semba H, Sawada H, Yamashita T. Intracardiac vortex intensity predicts early decompensation in dilated cardiomyopathy. Eur Heart J Cardiovasc Imaging 2016 17 (suppl 2): ii49-ii52.
3. Scali MC, Cortigiani L, De Nes M, Marzilli M, Picano E. The dynamic assessment of alveolar-capillary barrier during exercise echocardiography in heart failure patients with reduced ejection fraction. Eur Heart J Cardiovasc Imaging 2016 17 (suppl 2): ii37-ii45
4. Mast TP, Teske AJ, Walmsley J, Van Der Heijden JF, Van Es R, Prinzen F, et al. Echocardiographic deformation imaging and computer simulation for electromechanical substrate characterization in arrhythmogenic right ventricular cardiomyopathy. Eur Heart J Cardiovasc Imaging 2016 17 (suppl 2): ii69-ii70.
5. Lie OH, Saberniak J, Dejgaard LA, Anfinsen OG, Hegbom F, Edvardsen T, et al. How many are too many - frequent premature ventricular contractions and left ventricular function. Eur Heart J Cardiovasc Imaging 2016 17 (suppl 2): ii29-ii37
6. J J Hjertaas, K Matre. A twisting left ventricular ultrasound phantom for evaluation of 3D speckle tracking twist measurements. Eur Heart J Cardiovasc Imaging 2016; 17 (suppl 2): ii51
7. PB Bertrand, N Debusschere, T Dezutter, P Mortier, G De Santis , M Vrolix, et al. Patient specific numerical mitral valve modelling in secondary mitral regurgitation: clinical validity of a promising technique. Eur Heart J Cardiovasc Imaging 2016; 17(suppl 2): ii69
8. T E Chen , K Ong, RM Suri, M EnriqueSarano, HI Michelena, HM Burkhart, et al. Assessment of mitral annular physiology in myxomatous mitral disease with 3D transesophageal echocardiography: comparison between early severe mitral regurgitation and decompensated group. Eur Heart J Cardiovasc Imaging 2016; 17(suppl 2): ii108
9. V Boileve, J Dreyfus, D Attias, I Codogno, E Brochet, A Vahanian, et al. What causes mitral annulus dilatation? A three dimensional study. Eur Heart J Cardiovasc Imaging 2016; 17(suppl 2): ii253
10. E Surkova, J Bidviene, G Brunello, F Veronesi, G Cavalli, V Sokalskis, et al. Tricuspid annulus area correlates more with right atrial than right ventricular volumes in patients with different mechanisms of functional tricuspid regurgitation: a 3D echocardiography study. Eur Heart J Cardiovasc Imaging 2016; 17(suppl 2): ii16
11. E Cambronero Cortinas, J Grapsa, A Valle-Munoz, MJ Corbi-Pascual, W Gin-Sing, D Dawson, et al. Prognostic value of right atrial 3-dimensional speckle tracking in different

types of pulmonary arterial hypertension. Eur Heart J Cardiovasc Imaging 2016; 17(suppl 2): ii147

12. D Peluso, A Kovacs, E Surkova, D Muraru, M Perazzolo Marra, S Iliceto, et al. Importance of radial dysfunction to determine the impairment of right ventricular ejection fraction in patients with pulmonary hypertension. Eur Heart J Cardiovasc Imaging 2016; 17(suppl 2): ii162
13. S W Cho, SJ Park, SM Kim, JW Hwang, SA Chang, DS Jeong, et al. The validation and assessment of myocardial fibrosis by using cardiac magnetic resonance and speckle-tracking echocardiography in severe aortic stenosis. Eur Heart J Cardiovasc Imaging 2016; 17(suppl 2): ii150
14. K Gillis, G Bala, B Roosens, S Hernot, I Remory, S Droogmans, et al. Clinical validation of a semi-automatic quantification score of aortic valve calcification with ultrasound. Eur Heart J Cardiovasc Imaging 2016; 17(suppl 2): ii150
15. E Vitel, A Pimor, G Bouzille, C Leclercq, E Donal. Importance of the measurement of right ventricular function when exercising patients with asymptomatic severe primary mitral regurgitation. Eur Heart J Cardiovasc Imaging 2016; 17(suppl 2): ii69
16. A Mas-Stachurska, E Guasch, M Sitges, M Batlle, T Meirelles, N Castillo, et al. Impact of training on aortic and cardiac remodelling in a murine model of Marfan syndrome: an echocardiographic study. Eur Heart J Cardiovasc Imaging 2016; 17(suppl 2): ii71
17. G Di Salvo, N Al Qweai, Z Issa, N Muhanna, M Habdan, V Pergola, et al. Left ventricular mechanics in ALCAPA patients post successful repair: really normal? Eur Heart J Cardiovasc Imaging 2016; 17(suppl 2): ii256-ii263
18. MG Slieker, JM Meza, BW Mccrindle, T Karamlou, CI Tchervenkov, ML Jacobs, et al. Pre-intervention morphologic and functional echocardiographic characteristics of 651 neonates with critical left ventricular outflow tract obstruction. Eur Heart J Cardiovasc Imaging 2016; 17(suppl 2): ii71
19. B Bonello, M Carr, X Iriart, P Ciliberti, G Christov, I Sullivan, et al. Long term functional and myocardial assessment of patients with critical aortic valve stenosis. Eur Heart J Cardiovasc Imaging 2016; 17(suppl 2): ii72
20. L Almeida Morais, A Abreu, A Agapito, L De Sousa, J A Oliveira, A Viveiros Monteiro, et al. Exercise echocardiography value in the evaluation of operated aortic coarctation patients. Eur Heart J Cardiovasc Imaging 2016; 17(suppl 2): ii72
21. E Pagourelias, O Mirea, J Duchenne, W Budts, J Bogaert, M Gewillig, et al. Right ventricular remodelling after percutaneaous pulmonary valve replacement in corrected tetralogy of Fallot with severe pulmonary regurgitation.Time matters. Eur Heart J Cardiovasc Imaging 2016; 17(suppl 2): ii62
22. H Morillas Climent, A Osa Saez, O Cano Perez, D Domingo Valero, B Igual Munoz, L Martinez-Dolz, et al. Functional evolution of the right ventricle after pulmonary valve

replacement due to significant regurgitation. Implications in the surgical moment decision. Eur Heart J Cardiovasc Imaging 2016; 17(suppl 2): ii73

23. A Rosner, T Khalapyan, H Dalen, D Mc Elhinney, S Chen, C Haeffele, et al. Ventricular geometry and function in adult patients with Fontan surgery. Eur Heart J Cardiovasc Imaging 2016; 17(suppl 2): ii71
24. HJ Boiten, R Valkema, JC Van Den Berge, RT Van Domburg, F Zijlstra, AFL Schinkel. Impact of early coronary revascularization on longterm outcomes in patients with myocardial ischemia on myocardial perfusion single photon emission computed tomorgraphy. Eur Heart J Cardiovasc Imaging 2016; 17(suppl 2): ii56
25. F Valente, A RuizMunoz, L Galian, L Dux-Santoy, N Pizzi, S Aguade, et al. Dual energy computed tomography myocardial perfusion to detect coronary artery disease and predict need of revascularization. Eur Heart J Cardiovasc Imaging 2016; 17(suppl 2): ii56
26. J Duchenne, A Turco, P Claus, K Vunckx, J Nuyts, E Pagourelias, et al. Papillary muscles contribute significantly to shortening of dilated left ventricles. Eur Heart J Cardiovasc Imaging 2016; 17(suppl 2): ii53
27. S Pradel, S Brun, G Robin, G Victor, D Ribes, T Cognet, et al. Relationship between cardiac uptake by 99mTcDPD scintigraphy and left ventricular longitudinal strain in patients with transthyretinrelated cardiac amyloidosis. Eur Heart J Cardiovasc Imaging 2016; 17(suppl 2): ii53
28. LGW Grosse-Wortmann, PM Muthusami, ER Riesenkampff, DY Yim, RVDG Van Der Geest, MS Seed, et al. Quantitative perfusion and extracellular volume after Kawasaki disease in children: tissue assessment beyond late gadolinium enhancement by cardiac MRI. Eur Heart J Cardiovasc Imaging 2016; 17(suppl 2): ii63
29. L Dux-Santoy, JF Rodriguez-Palomares, R Kale, G Maldonado, F Valente, G Teixido-Tura, et al. Three-dimensional wall shear stress assessed by 4Dflow CMR in bicuspid aortic valve disease. Eur Heart J Cardiovasc Imaging 2016; 17(suppl 2): ii63
30. L Dux-Santoy, JF Rodriguez-Palomares, R Kale, G Maldonado, F Valente, G Teixido-Tura, et al. Flow patterns and rotational flow as predictors of ascending aorta dilatation in bicuspid aortic valve. Eur Heart J Cardiovasc Imaging 2016; 17(suppl 2): ii63
31. R Hinojar, C Fernandez-Golfin, A Gonzalez-Gomez, A Esteban, M Plaza Martin, MA Fernandez-Mendez, et al. Normal values left atrial strain using cardiovascular magnetic resonance feature tracking. Eur Heart J Cardiovasc Imaging 2016; 17(suppl 2): ii64